ECCOMAS Congress 2016
VII European Congress on Computational Methods in Applied Sciences and Engineering
M. Papadrakakis, V. Papadopoulos, G. Stefanou, V. Plevris (eds.)
Crete Island, Greece, 5–10 June 2016

EQUIVALENT UNIAXIAL ACCELEROGRAM FOR CSS-BASED ISOLATION SYSTEMS ASSESSMENT UNDER TWO-COMPONENTS SEISMIC EVENTS

M. Furinghetti[1], **A. Pavese**[2]

[1] EUCENTRE - Pavia
via Ferrata 1, 27100 Pavia - Italy
e-mail: marco.furinghetti@eucentre.it

[2] University of Pavia
via Ferrata 1, 27100 Pavia - Italy
a.pavese@unipv.it

Keywords: Concave Surface Slider, bi-axial interaction, frictional force, equivalent uniaxial accelerogram, bi-directional motion, base-isolation.

Abstract. *Concave Surface Slider (CSS) devices represent an effective solution for base-isolation design problems. In such isolators the energy dissipation capability is induced by the sliding motions which occur at one or more sliding interfaces. The spherical shape of the sliding surfaces provides a significant recentering behavior, by means of the stepwise projection of the applied vertical load with respect to both horizontal directions. One of the most important assumptions states that the lateral response of a CSS device can be considered as the direct summation of the recentering force and the frictional force. For two-components earthquake excitations, the recentering force is computed as a linear spring with respect to displacements along the main directions of motion; whereas, the frictional response is returned by the stepwise projection of the total frictional force, which is aligned with respect to the trajectory of the device: thus, a bi-axial interaction of the directions of motion has to be accounted for, when a friction-based device is modelled. However, available commercial software which can capture such a behavior are limited. In this work an analytical procedure is defined, for the computation of an "equivalent uniaxial accelerogram" for the seismic assessment of a base-isolated structure, subjected to a bi-directional earthquake. Thanks to the proposed theory, it is possible to compute a single ground acceleration time-history, related to a proper direction angle, which can reproduce the same effects of a two-components seismic event on a base-isolated structural system: the analogy between the equivalent uniaxial and the bi-directional events has been studied in terms of acceleration, velocity and displacement spectra respectively. Results for the base-isolated structure have been analyzed in terms of displacement, absolute acceleration and interstorey shear responses.*

1 INTRODUCTION

Concave Surface Slider (CSS) devices are widely used in real applications for seismic vulnerability mitigation all over the world. Thanks to the easy geometric and mechanical definition of such isolators, it is possible to achieve high values of dissipated energy and, consequently, lower internal forces are induced into the superstructure during the seismic event [10]. Nonetheless, a lot of research, both numerical and experimental, has been developed in last years, aiming at getting a better understanding of the lateral response characteristics of friction-based devices [3, 6]. One of the key points of the behavior of CSS isolators is represented by the frictional response under bi-directional seismic events [4, 6, 8]. Generally, the force response of a CSS device can be considered as the direct summation of a recentering force and a frictional force. The recentering contribution can be modelled as a linear spring with respect to displacements along both x and y directions, whereas the frictional force is a complicated function of vertical load, sliding velocity and cyclic effects, and it is parallel to the trajectory of the device [1]. Thus, the main frictional force has to be stepwise projected along the main directions of the reference system, and a bi-axial interaction has to be considered. This aspect has been noticed in experimental results as well as in analytical simulations [3, 5]. In Figure 1 the analytical hysteretic responses along x and y directions of a single device subjected to a cloverleaf displacement trajectory are shown (friction coefficient: 7% ; Equivalent radius of curvature: 3.1m).

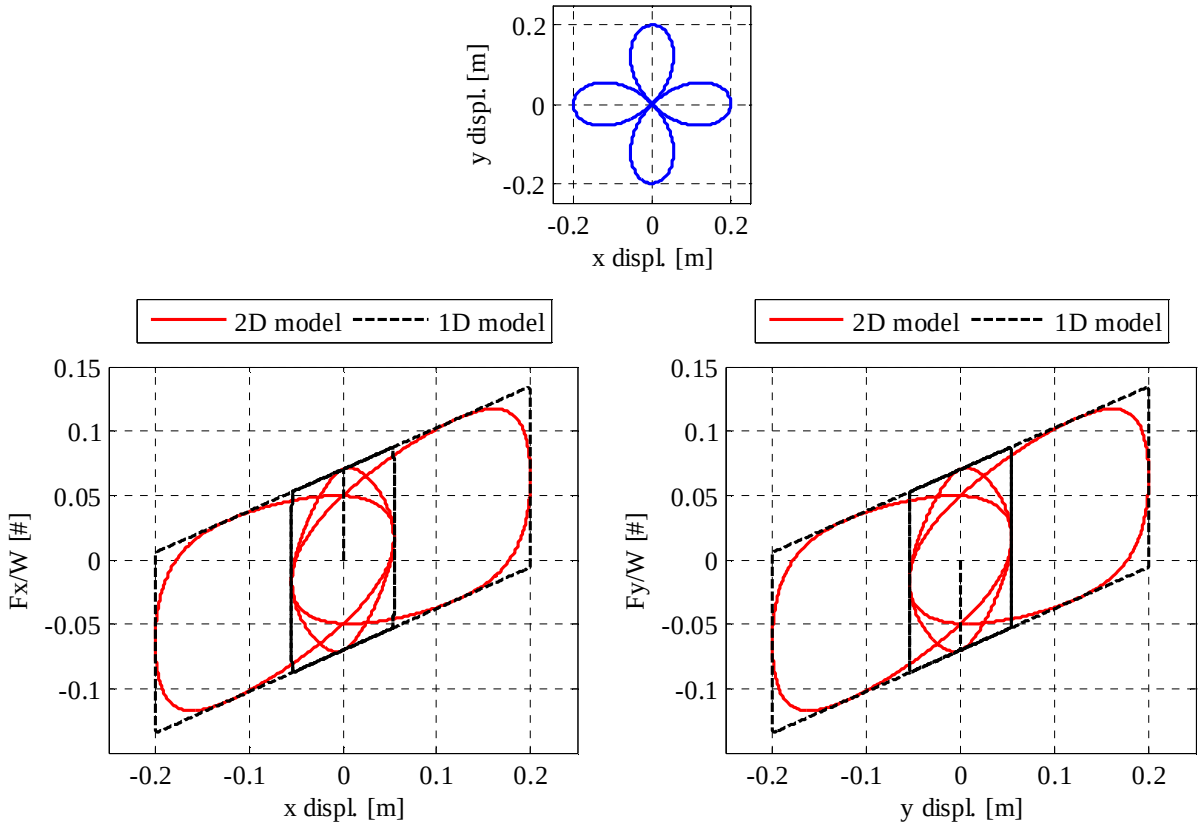

Figure 1: Analytical simulation the CSS hysteretic response under a cloverleaf trajectory.

It can be noted that by accounting for bi-axial interaction of the directions of motion, the maximum force value decreases along both x and y directions, due to the changing in orientation of the main frictional force during motion, in comparison to the unidirectional model, which considers the frictional force parallel to the recentering one at each time step. Hence,

the seismic response of a base-isolated structure can be strongly affected by the bi-axial interaction of the directions of motion. However, most of the design and verification procedures are based on simplified unidirectional approaches [9]; moreover, testing protocols for such a kind of devices mainly consist of unidirectional tests, according to UNI:EN15129 standard code [7], and bidirectional tests can be substituted by a unidirectional motion along an orthogonal direction. Furthermore, only recent versions of commercial softwares can model such behavior, and significantly high run times may be experienced.

In this work an analytical procedure is presented, which can return an equivalent uniaxial accelerogram representative of a bi-directional seismic event. Thanks to the present theory, it is possible to apply a uni-directional radial motion to the structure, for the evaluation of structural internal forces and displacements under a general bi-directional earthquake. Results of a base-isolated building structure have shown a good agreement of the response under the equivalent uniaxial event in comparison to the bi-axial one, in terms of displacement, absolute acceleration and interstorey shear values.

2 EQUIVALENT UNIAXIAL EVENT

In this section the presented procedure for the computation of the equivalent uniaxial event of a bidirectional earthquake is reported.

Generally, a bidirectional seismic event is represented by two individual ground acceleration time-series along x and y directions respectively, where x and y are plan orthogonal directions of the reference system of the analyzed structure. Since there are a lot of aspects which influence the propagation of seismic waves during an earthquake (such as rupture mechanism, soil mechanical characteristics, topographic and stratigraphic distributions, etc…), the resulting diagram which represents both the ground acceleration time series together, that is $\ddot{y}_g$ vs. $\ddot{x}_g$, consists of a scatter plot of acceleration points, and no preferential direction of motion can be immediately detected. In Figure 2 the ground acceleration diagram related to the Irpinia earthquake 1980 is reported.

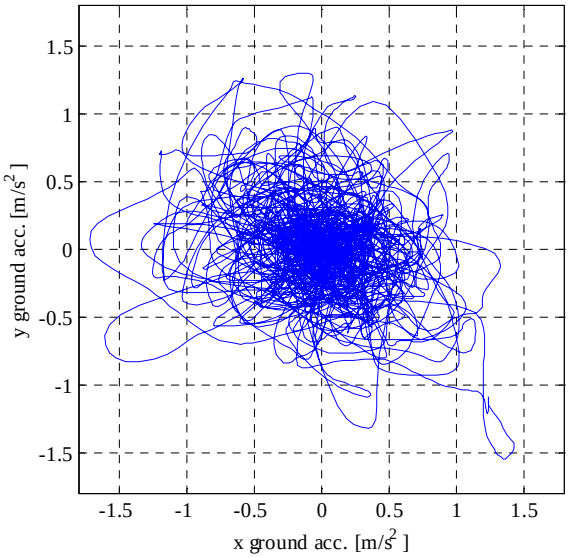

Figure 2: Irpinia earthquake 1980 – Ground acceleration diagram.

Thus, the response spectrum of the seismic event has to be considered. A response spectrum of the bi-directional event has been defined, by means of the direct integration of the

equations of motion along both x and y directions of a linear single oscillator with different values of structural periods T and for a given damping ratio ξ:

$$\begin{aligned} \ddot{x} + 2\xi\omega\dot{x} + \omega^2 x &= -\ddot{x}_g \\ \ddot{y} + 2\xi\omega\dot{y} + \omega^2 y &= -\ddot{y}_g \end{aligned} \tag{1}$$

Hence, the maximum vectorial displacement and absolute acceleration are detected.

$$\begin{aligned} S_d^{2D}(\xi, T) &= \max\left(\sqrt{x^2 + y^2}\right) \\ S_a^{2D}(\xi, T) &= \max\left(\sqrt{\left(\ddot{x} + \ddot{x}_g\right)^2 + \left(\ddot{y} + \ddot{y}_g\right)^2}\right) \end{aligned} \tag{2}$$

By considering several period values, the reference response spectrum related to the bidirectional earthquake is finally obtained. Therefore, for a given direction angle, the projection of each acceleration point shown in Figure 2 is obtained, in order to compute a single ground acceleration component along the considered direction. In Figure 3 the projection procedure is reported.

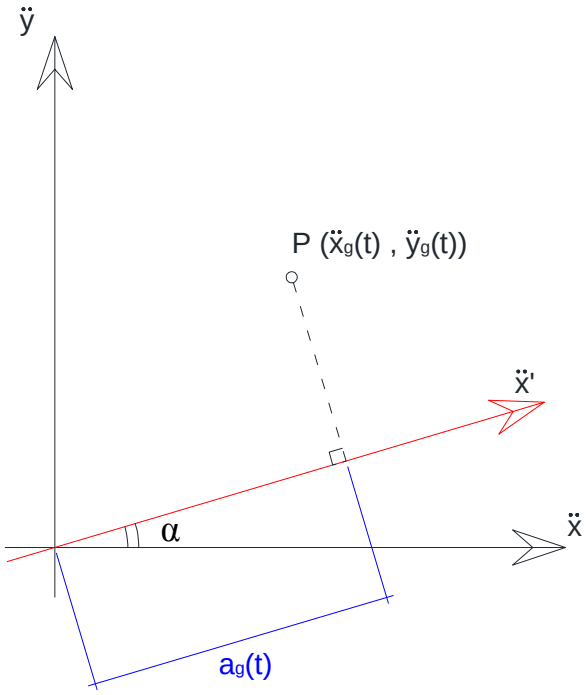

Figure 3: Equivalent uniaxial event – Projection procedure.

According to the aforementioned scheme, the uniaxial projection of the bidirectional earthquake $a_g(t)$ is defined for the given orientation α as follows:

$$a_g(t) = \ddot{x}_g(t)\cos(\alpha) + \ddot{y}_g(t)\sin(\alpha) \tag{3}$$

Consequently, the ordinary 1D acceleration and displacement response spectra associated to $a_g(t)$ can be obtained, by assuming the same damping ratio of the reference 2D response spectrum. Then, a parameter which describes the discrepancies between the reference 2D and the 1D response spectra is defined, by computing the square root of the Mean Squared Error:

such a parameter can be computed by considering either the acceleration or the displacement response spectrum; both the approaches have been evaluated for sake of comparison.

$$E^{S_d}(\xi,\alpha) = \sqrt{MSE^{S_d}} = \sqrt{\frac{1}{n_T}\sum_{i=1}^{n_T}\left(S_d^{2D}(\xi,T_i) - S_d^{1D}(\xi,\alpha,T_i)\right)^2}$$
$$E^{S_a}(\xi,\alpha) = \sqrt{MSE^{S_a}} = \sqrt{\frac{1}{n_T}\sum_{i=1}^{n_T}\left(S_a^{2D}(\xi,T_i) - S_a^{1D}(\xi,\alpha,T_i)\right)^2} \quad (4)$$

Where n_T is the total number of structural periods, considered for the computation of the response spectra. Finally, by considering the direction angle α within a range between 0° and 180°, the optimum direction angle which returns the minimum error parameter can be obtained. In Figure 4 and Figure 5 the aforementioned procedure has been applied to the Irpinia earthquake 1980, by considering a damping ratio equal to 5% and acceleration and displacement spectra respectively.

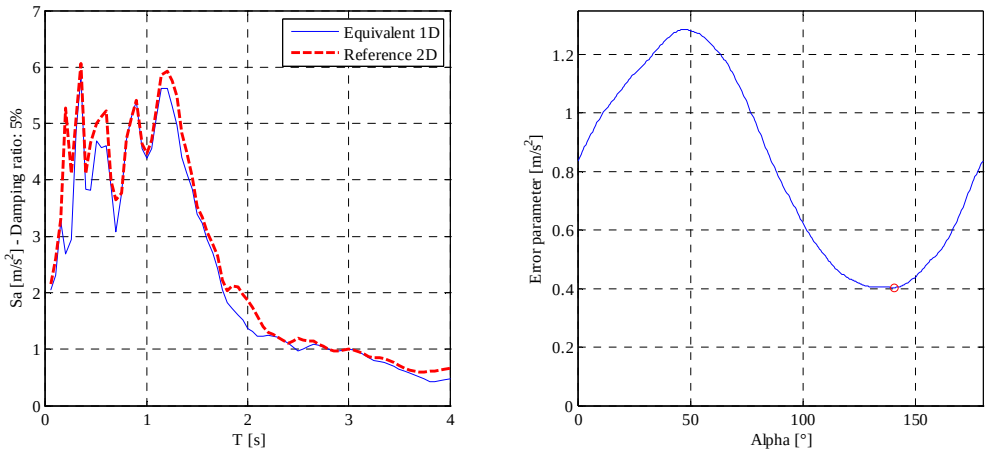

Figure 4: Equivalent uniaxial event – Irpinia earthquake – acceleration-based procedure.

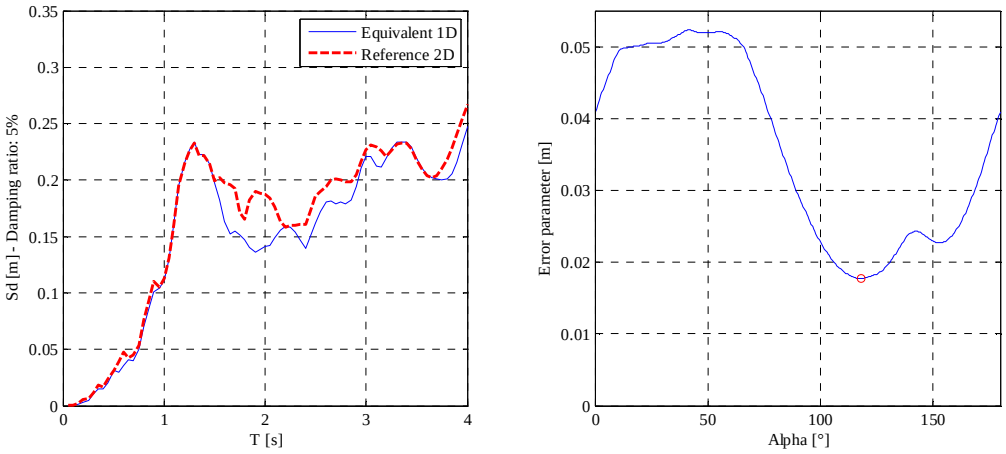

Figure 5: Equivalent uniaxial event – Irpinia earthquake – displacement-based procedure.

In what follows results for three different bidirectional earthquakes are reported, by varying the damping ratio; the analyzed seismic events are listed in Table 1.

Event #	Location	Year	Mw	PGA_x [m/s^2]	PGA_y [m/s^2]
1	Irpinia	1980	6.9	1.718	1.550
2	Emilia	2012	6.1	2.574	2.591
3	L'Aquila	2009	6.3	6.442	5.352

Table 1: Equivalent uniaxial event – seismic events characteristics.

Results are shown in terms of both optimum direction angle and error parameter values as a function of the damping ratio. In Figure 6 and Figure 7 results are shown, by considering acceleration and displacement error respectively.

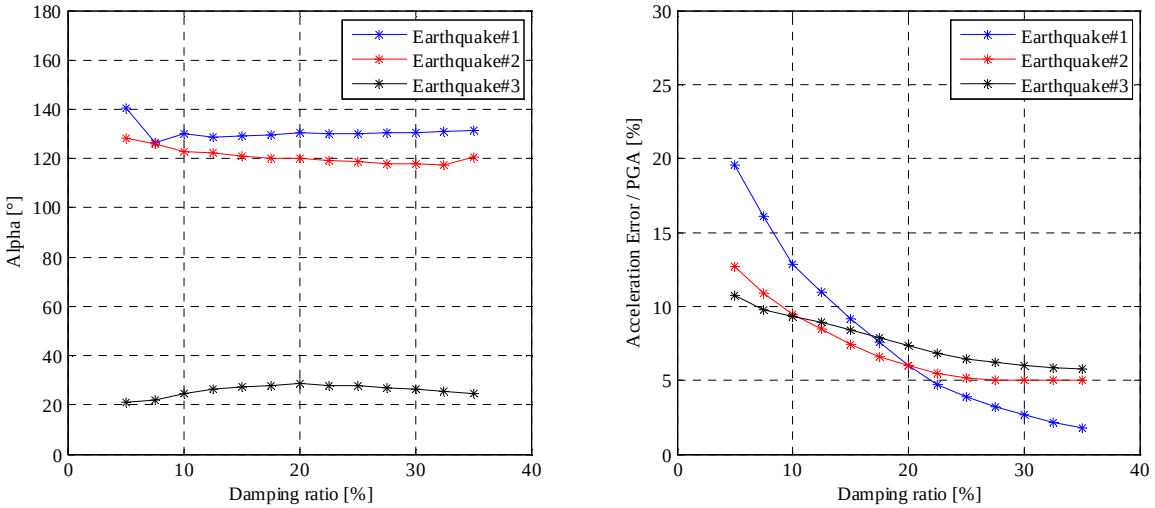

Figure 6: Equivalent uniaxial event – damping analysis – acceleration-based procedure.

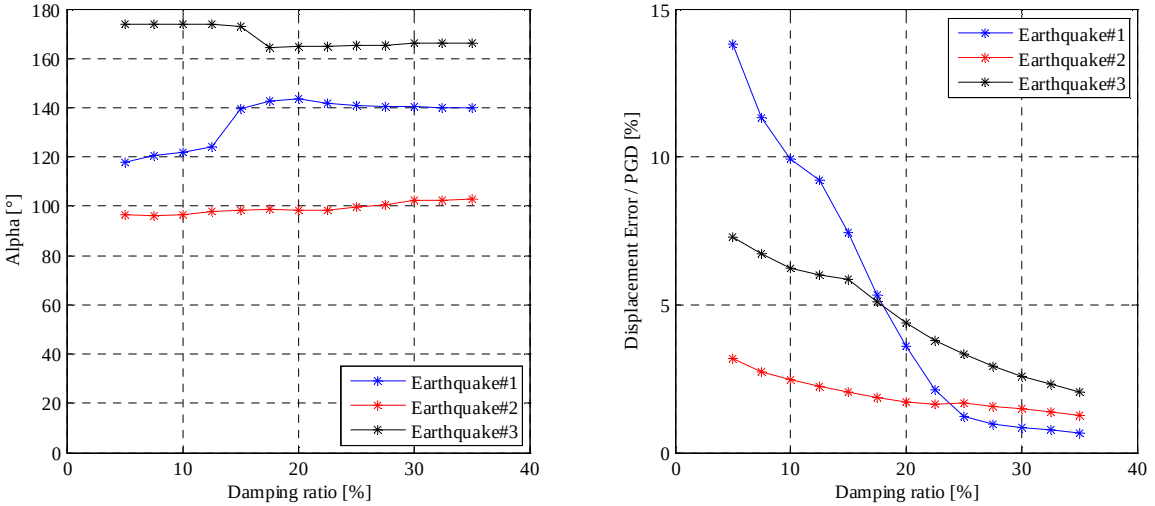

Figure 7: Equivalent uniaxial event – damping analysis – displacement-based procedure.

It can be noted that the acceleration spectrum approach leads to more stable results, in terms of optimum direction angle value, which can be considered approximately constant with respect to increasing values of damping ratio; in addition, as the damping ratio increases, the acceleration error parameter significantly decreases, and a similar decay trend of the acceleration error has been found among the considered earthquakes. On the other hand, the dis-

placement-based procedure returns more irregular results: the optimum variation angle value can be affected by the damping ratio and, decreasing trend of the displacement error parameter is found at high values of damping ratio as well as for the acceleration procedure.

3 ANALYTICAL MODEL DEFINITION

In this endeavor the structural model presented in Furinghetti and Pavese 2015 has been used [4], which consists of a Multi Degrees Of Freedom (MDOF) scheme, base-isolated by means of an equivalent CSS device, which is representative of the entire isolation system (Figure 8).

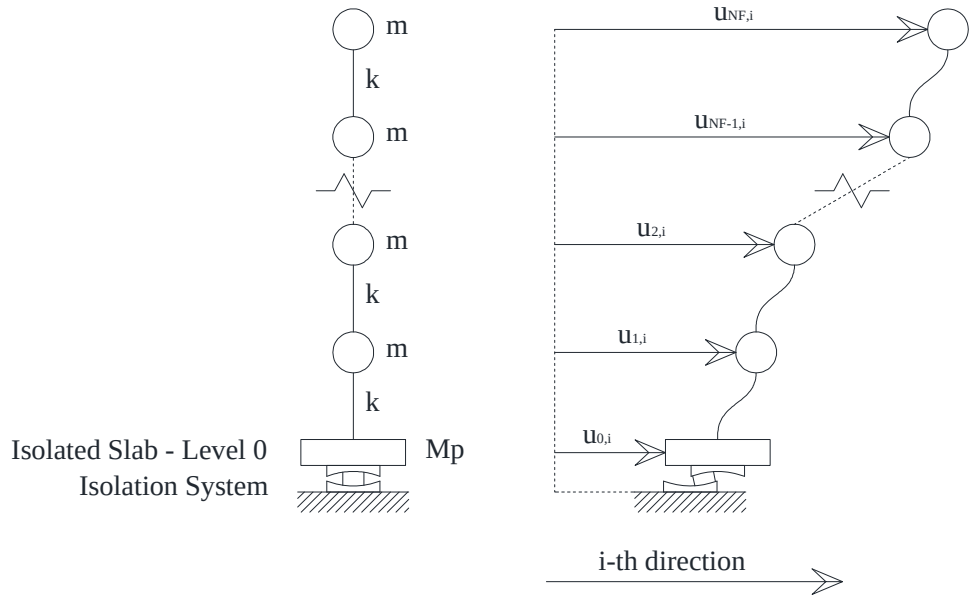

Figure 8: Dynamic model of the isolated structure.

This assumption can be adopted when a building with a large plan development is considered. Thus, all the isolators have averagely the same vertical load, directly equal to the total weight of the isolated structure divided by the number of devices. Hence, the horizontal force along both x and y directions of the isolation system can be computed as follows:

$$\frac{F_{is}}{m} = g \cdot N_F \cdot \left(1+\frac{1}{r}\right) \cdot \left\{ \frac{1}{R_{eq}} \begin{bmatrix} u_{0,x} \\ u_{0,y} \end{bmatrix} + \mu(W, v, E) \cdot \tanh\left(\frac{v}{v_s}\right) \cdot \begin{bmatrix} \dfrac{\dot{u}_{0,x}}{\sqrt{(\dot{u}_{0,x})^2 + (\dot{u}_{0,y})^2}} \\ \dfrac{\dot{u}_{0,y}}{\sqrt{(\dot{u}_{0,x})^2 + (\dot{u}_{0,y})^2}} \end{bmatrix} \right\}$$

being (5)

$$\frac{W_{tot}}{m} = \frac{g}{m} \cdot \left(M_B + M_P\right) = \frac{g}{m} \cdot M_B \cdot \left(1+\frac{M_P}{M_B}\right) = \frac{g}{m} \cdot M_B \cdot \left(1+\frac{1}{r}\right) = g \cdot N_F \cdot \left(1+\frac{1}{r}\right)$$

Where M_B is the total mass of the building, and M_P is the mass of the isolated plate. Finally, the normalized dynamic system of the isolated structure is consequently defined for direction

i = x, y. The contribution of the isolation system has to be added in the first equation only for both directions, which represents the translational dynamic equilibrium of the isolated slab.

$$\left[\frac{M_{tot}}{m}\right]\begin{pmatrix}\ddot{u}_{0,i}\\ \hline \ddot{u}_{1,i}\\ \ddot{u}_{2,i}\\ \vdots\\ \ddot{u}_{N_F,i}\end{pmatrix}+\left[\frac{C_{tot}}{m}\right]\begin{pmatrix}0\\ \hline \dot{u}_{1,i}-\dot{u}_{0,i}\\ \dot{u}_{2,i}-\dot{u}_{0,i}\\ \vdots\\ \dot{u}_{N_F,i}-\dot{u}_{0,i}\end{pmatrix}+\left[\frac{K_{tot}}{m}\right]\begin{pmatrix}u_{0,i}\\ \hline u_{1,i}\\ u_{2,i}\\ \vdots\\ u_{N_F,i}\end{pmatrix}+\frac{F_{is,i}}{m}\begin{pmatrix}1\\ 0\\ 0\\ \vdots\\ 0\end{pmatrix}=-\left[\frac{M_{tot}}{m}\right]\cdot\ddot{u}_{g,i} \qquad (6)$$

The damping matrix is obtained by accounting for Rayleigh damping, with a target damping ratio equal to 5% [11].

4 CASE STUDY STRUCTURE AND SEISMIC INPUT

The case study building consists of a three storey R.C. frame structure, with a total mass equal to 2048 tons [2], which is base-isolated by means of CSS devices, and a R.C. isolated slab with a thickness of 0.5m, as shown in Figure 9.

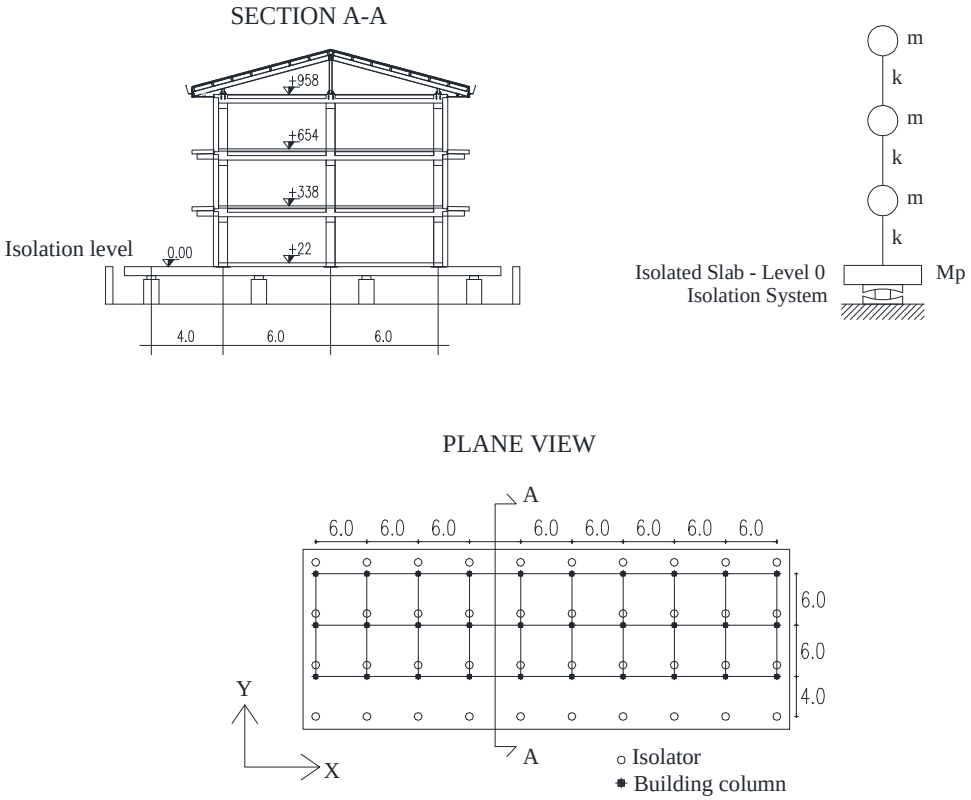

Figure 9: Case study structure.

The isolated plate has a total mass equal to 1496 tons: thus, according to the aforementioned analytical model, the ratio between the masses of the building and the isolated plate is equal to 1,37. The first mode period is equal to 0,48s and a target damping ratio of 5% has been set for all the modes. CSS devices have been modelled with a an equivalent radius of curvature equal to 3,1m; furthermore, in this work the friction coefficient has been considered

as a constant function of vertical load, sliding velocity and dissipated energy: the numerical value is equal to 7% [3, 4].

For what concerns the input signals, all the previously analyzed earthquakes have been applied to the case study structure. Since the displacement demand and the associated hysteretic damping ratio is not a priori known, for all the bi-directional earthquakes the optimum direction angle of the equivalent uniaxial event has been computed with a damping ratio equal to 5% and both acceleration and displacement approaches have been processed. In Table 2 the characteristics of the seismic events are listed.

Event #	Location	Scale factor	1D angle [°] acc. approach	1D angle [°] displ. approach
1	Irpinia	1.5	140.5	118.0
2	Emilia	1.5	128.0	94.5
3	L'Aquila	1.5	21.0	179.5

Table 2: Case study– seismic events characteristics.

A scale factor for both x and y components equal to 1.5 has been used for all the considered seismic events, in order to achieve a maximum displacement demand comparable to the design displacement capacity of the devices.

5 ANALYSES RESULTS

In the followings the results are shown in terms of displacement, absolute acceleration and interstorey shear profiles of the case study structure, subjected to the bidirectional event in comparison to the equivalent uniaxial cases.

In Figure 10 , Figure 11 and Figure 12 displacement results are reported for earthquake #1, #2 and #3 respectively, and by accounting for acceleration (left) rather than displacement (right) approach.

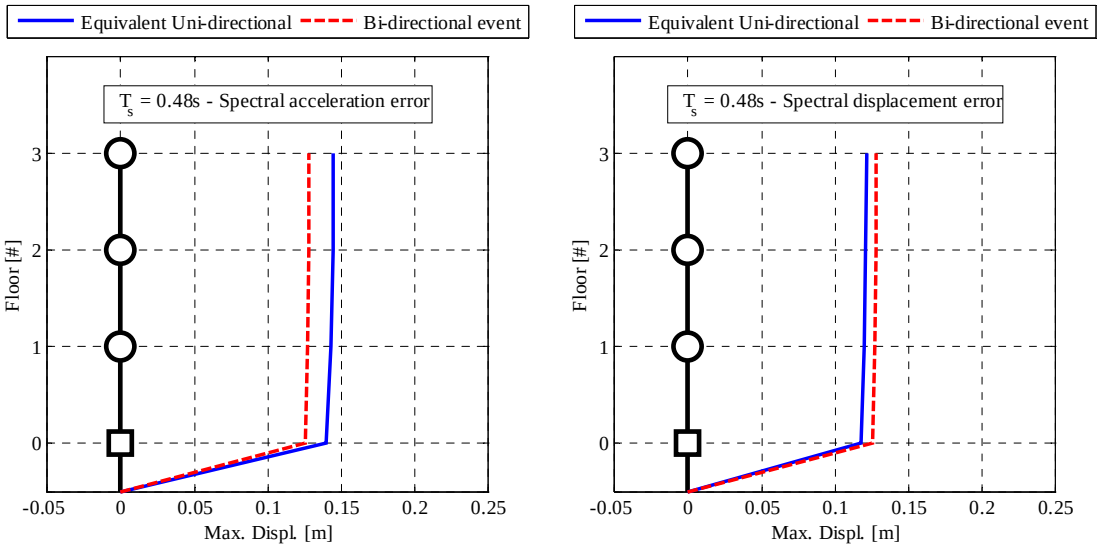

Figure 10: Results – Eqk#1 – displacement profiles.

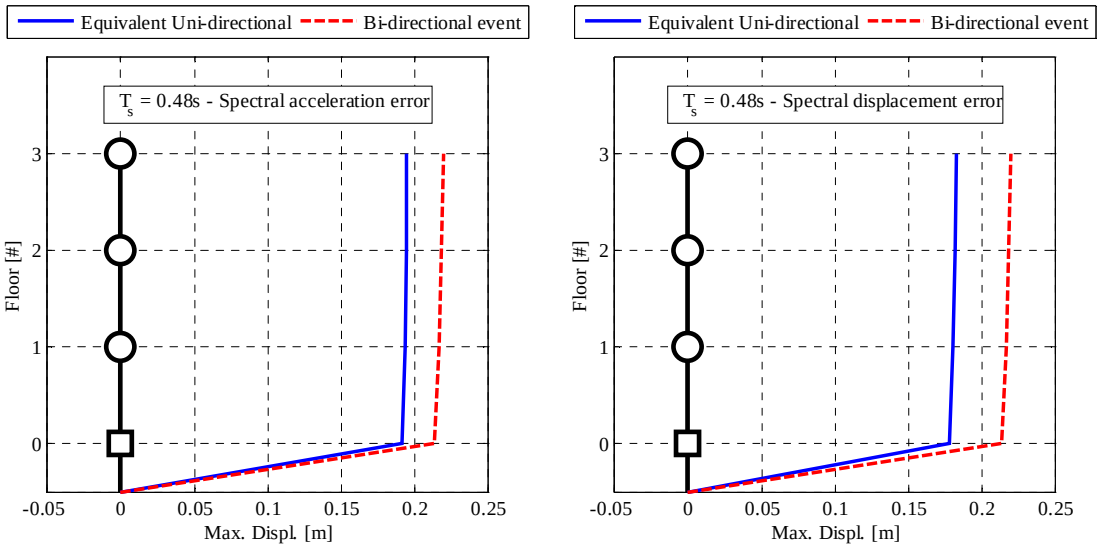

Figure 11: Results – Eqk#2 – displacement profiles.

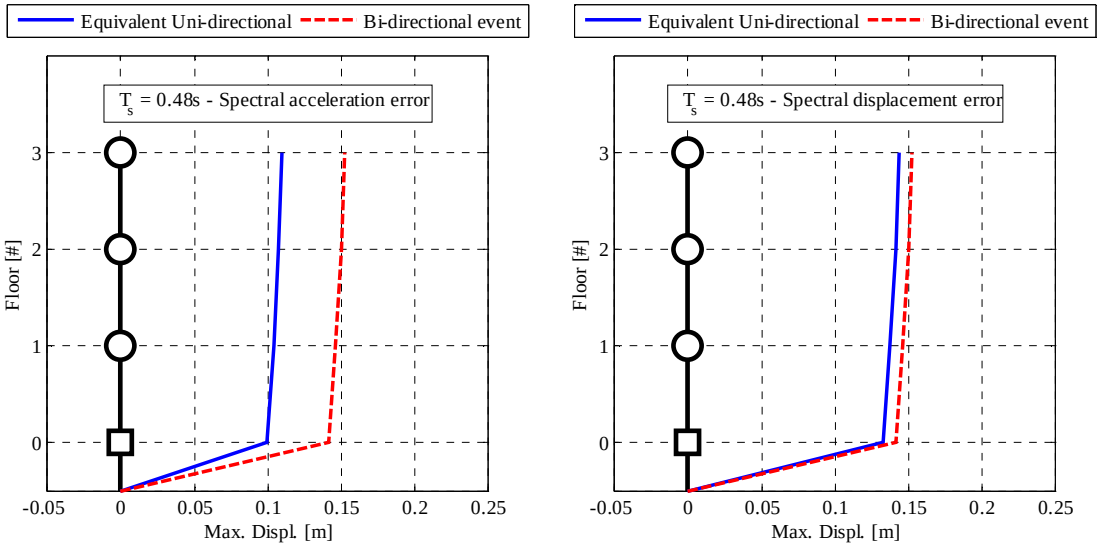

Figure 12: Results – Eqk#3 – displacement profiles.

In Table 3 the variation percentages at all levels of the displacement demand related to the equivalent uniaxial earthquake in comparison to the biaxial seismic event.

	Eqrthquake #1		Eqrthquake #2		Eqrthquake #3	
Level #	Acc. approach	Displ. approach	Acc. approach	Displ. approach	Acc. approach	Displ. approach
0	11.9%	-6.3%	-10.7%	-17.0%	-29.6%	-6.0%
1	12.4%	-5.8%	-10.8%	-16.8%	-28.7%	-5.8%
2	13.0%	-5.3%	-11.1%	-16.8%	-28.2%	-5.7%
3	13.3%	-5.0%	-11.4%	-16.8%	-28.1%	-5.6%

Table 3: Results – Variation percentages – displacement response.

As can be noted, for earthquake #1 and #3 the best agreement is achieved by using the displacement spectrum approach, whereas for the second earthquake the direction angle returned by the acceleration procedure leads to better results. Generally, the displacement demand decreases at all levels, if the equivalent uniaxial event is considered; only for earthquake #1 with acceleration approach opposite evidences have been found.

In Figure 13 , Figure 14 and Figure 15 absolute acceleration results are reported for earthquake #1, #2 and #3 respectively, and by accounting for acceleration (left) rather than displacement (right) approach.

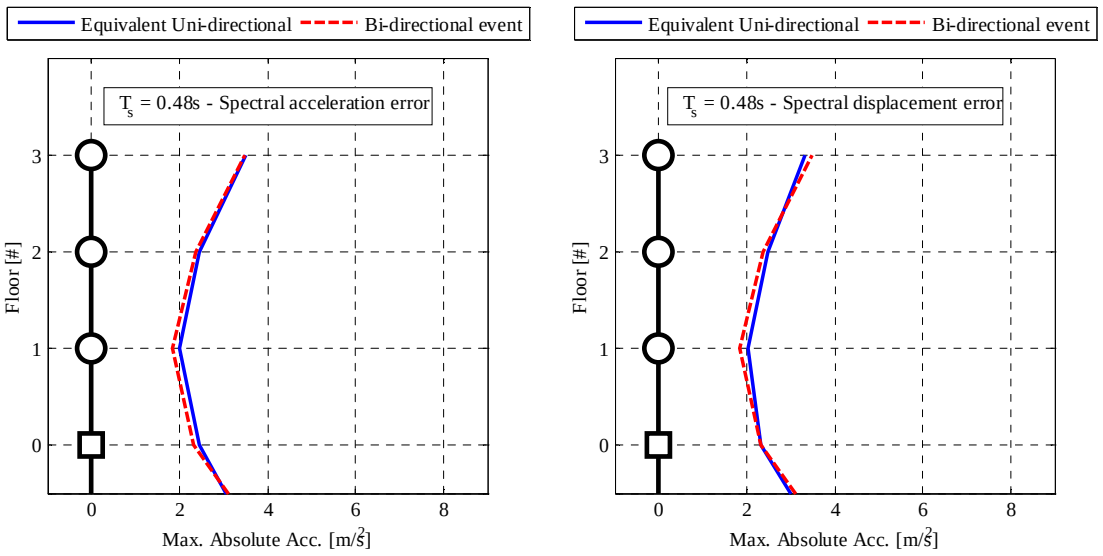

Figure 13: Results – Eqk#1 – absolute acceleration profiles.

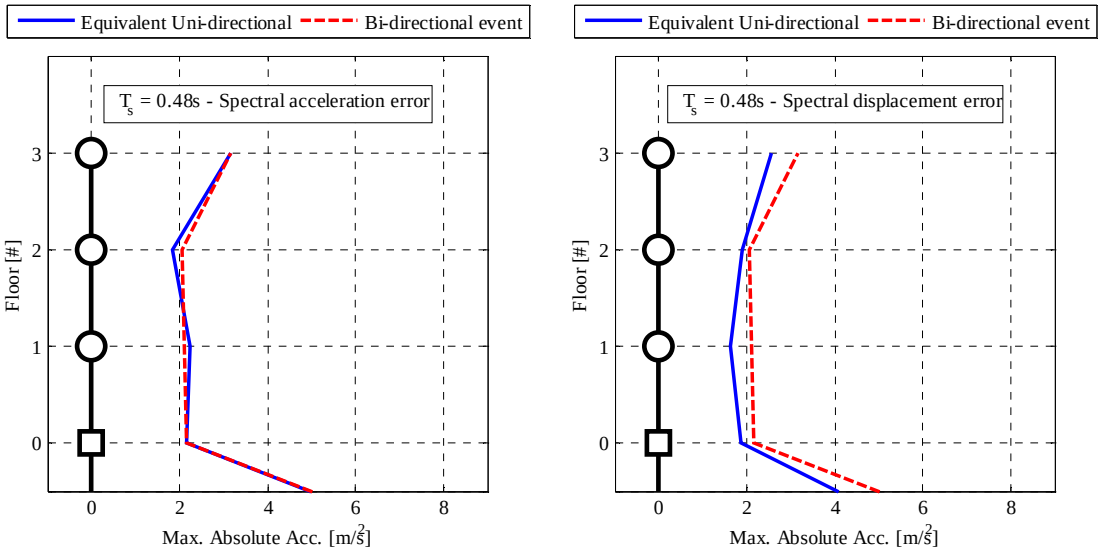

Figure 14: Results – Eqk#2 – absolute acceleration profiles.

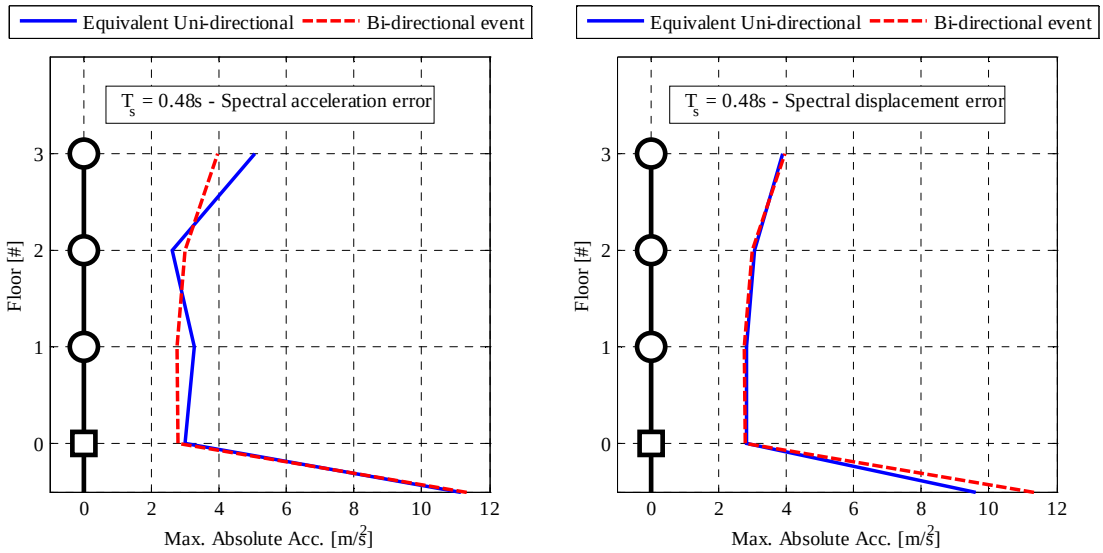

Figure 15: Results – Eqk#3 – absolute acceleration profiles.

In Table 4 the variation percentages at all levels of the absolute acceleration demand related to the equivalent uniaxial earthquake in comparison to the biaxial seismic event.

	Eqrthquake #1		Eqrthquake #2		Eqrthquake #3	
Level #	Acc. approach	Displ. approach	Acc. approach	Displ. approach	Acc. approach	Displ. approach
0	4.8%	0.0%	0.3%	-13.1%	7.5%	0.9%
1	7.9%	9.0%	6.0%	-22.5%	17.6%	2.3%
2	3.9%	4.3%	-10.1%	-7.9%	-12.2%	2.6%
3	0.7%	-4.8%	0.1%	-19.1%	28.2%	-1.4%

Table 4: Results – Variation percentages – absolute acceleration response.

In all cases acceleration profiles relative to the biaxial seismic event are almost overlapped to the ones associated to the equivalent uniaxial earthquake: thus, even though 5% damping is assumed for the computation of the optimum direction angle for both displacement and acceleration approaches, the acceleration response can be properly captured by applying an equivalent radial motion. For eqk#1 and #2 the best comparison is obtained by accounting for the acceleration procedure, whereas for eqk#3 the displacement approach provides a better estimates of the bidirectional acceleration profile.

In Figure 16 , Figure 17 and Figure 18 interstorey shear results are reported for earthquake #1, #2 and #3 respectively, and by accounting for acceleration (left) rather than displacement (right) approach.

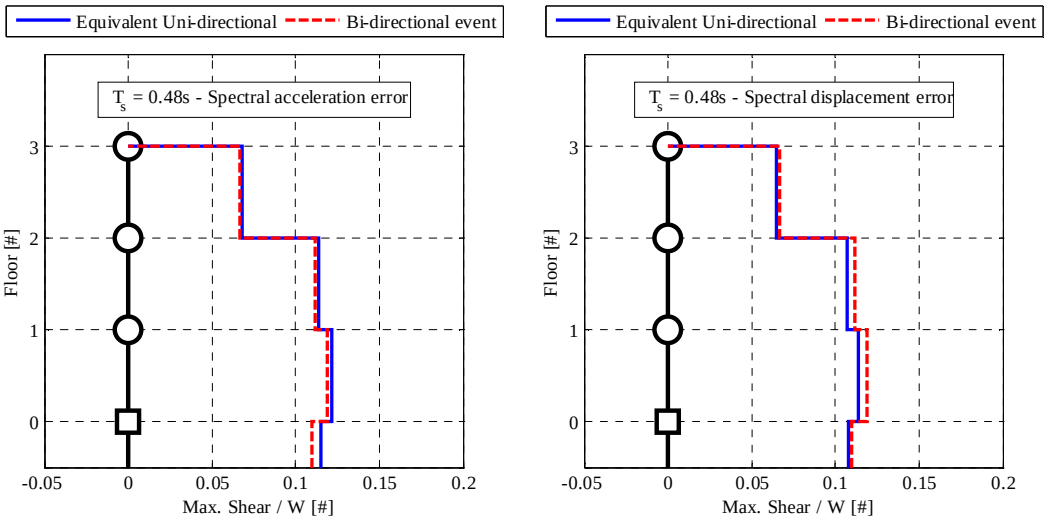

Figure 16: Results – Eqk#1 – interstorey shear profiles.

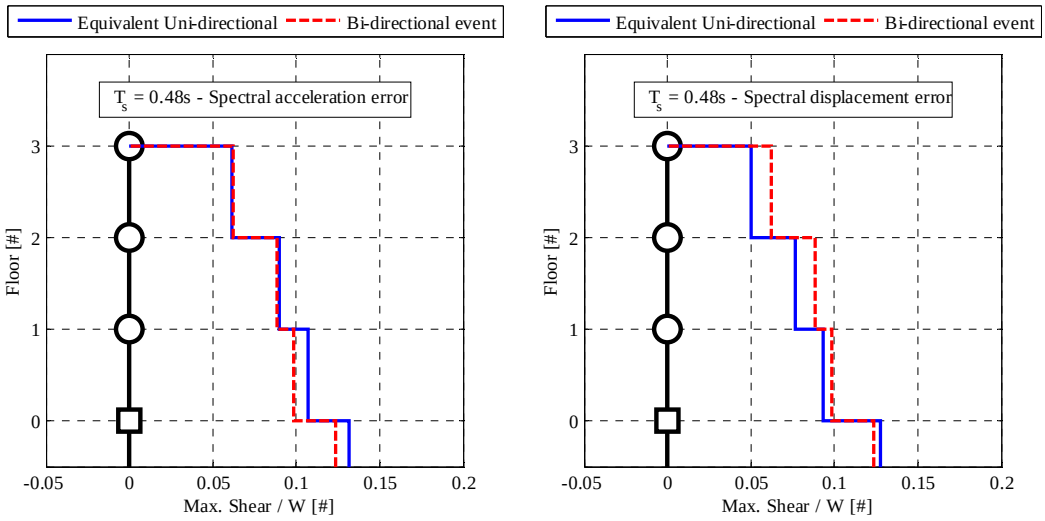

Figure 17: Results – Eqk#2 – interstorey shear profiles.

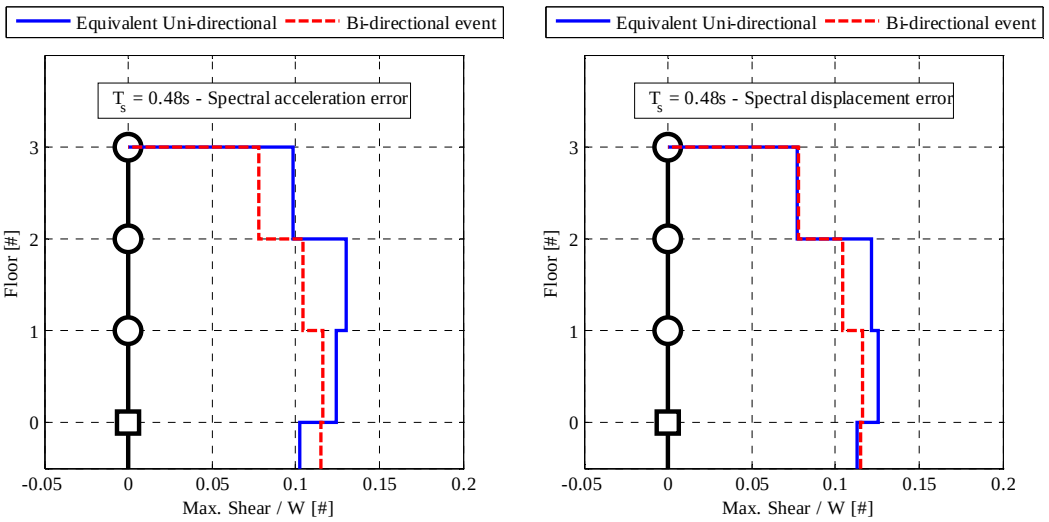

Figure 18: Results – Eqk#3 – interstorey shear profiles.

In Table 5 the variation percentages at all levels of the interstorey shear demand related to the equivalent uniaxial earthquake in comparison to the biaxial seismic event.

	Eqrthquake #1		Eqrthquake #2		Eqrthquake #3	
Level #	Acc. approach	Displ. approach	Acc. approach	Displ. approach	Acc. approach	Displ. approach
0	5.1%	-1.6%	6.8%	3.3%	-11.1%	-1.7%
1	2.2%	-4.3%	8.8%	-4.9%	6.5%	7.7%
2	2.1%	-4.1%	1.4%	-13.4%	25.0%	16.6%
3	1.9%	-2.9%	-1.1%	-19.2%	26.4%	-1.1%

Table 5: Results – Variation percentages – interstorey shear response.

Also concerning shear profiles, the equivalent unidirectional event provides a good estimate of the bidirectional response at all levels. Again, the acceleration procedure leads to better results for eqk#1 and #2.

6 CONCLUSIONS AND FUTURE DEVELOPMENTS

In this work an analytical procedure for the computation of an equivalent uniaxial seismic event for a bidirectional earthquake is presented. Such a procedure allows to compute the optimum direction angle of the equivalent radial motion, by projecting along several directions all the acceleration points of the bidirectional earthquake and evaluating the associated error parameter between the biaxial and the uniaxial response spectrum; both acceleration and displacement response spectra have been considered. Three different bidirectional seismic events have been studied and then applied to a case study base-isolated structure, in order to underline differences between the biaxial and the equivalent uniaxial responses, in terms of displacement, absolute acceleration and interstorey shear demands.

For the analyzed earthquakes it has been noticed that the optimum direction angle can be approximately considered constant with respect to the damping ratio and the error parameter significantly decreases with increasing values of damping ratio, if the acceleration spectrum approach is used; on the other hand the displacement approach leads to more irregular results.

Concerning structural responses, displacement demands at all levels are underestimated when the equivalent uniaxial earthquake is applied, exception made for earthquake #1, with acceleration approach. The best approximation is returned by the acceleration approach, which leads to variations in the range between 5% and 15%, whereas higher variations can be experienced with displacement approach. Regarding absolute acceleration responses, a good agreement between biaxial and equivalent uniaxial events is reached with both the approaches, even though in most of the cases the lowest variations can be found with the acceleration-based procedure (less than 10%). Similar conclusions can be drawn also for interstorey shear responses.

Future developments of the present work will consist of a wide numerical study on a real application, modelled with a commonly used commercial software, in order to underline influences in the main response parameters of the effective horizontal and vertical spatial distribution of the structural elements, by accounting for both biaxial and equivalent uniaxial earthquakes; furthermore, a wider set of seismic events will be analyzed, aiming at generalizing all the previously discussed aspects.

REFERENCES

[1] M. Furinghetti, C. Casarotti, A. Pavese, Effects of bi-directional motion on a structural system isolated with DCSS devices with laying defects. *15th WCEE, World Conference on Earthquake Engineering*, Lisbon, Portugal, September 24-28, 2012.

[2] C. Casarotti, M. Furinghetti, A. Pavese, Evaluation of response of an isolated system based on Double Curved Surface Slider. *Computational method in Earthquake Engineering*, **30**, pp 397-416, 2013.

[3] M. Furinghetti, C. Casarotti, A. Pavese, Bi-directional experimental response of full scale DCSS devices. *2ECEES, Second European Conference on Earthquake Engineering and Seismology*, Istanbul, Turkey, August 25-29, 2014.

[4] M. Furinghetti, A. Pavese, Numerical Assessment on the Seismic Response of a Base-Isolated Building under Bi-Directional Motion. *5th ECCOMAS Thematic Conference on Computational Methods in Structural Dynamics and Earthquake Engineering*, Crete Island, Greece, May 25-27, 2015.

[5] G. Lomiento, N. Bonessio, G. Benzoni, Concave sliding isolator's performance under multi-directional excitation. *Ingegneria Sismica*, **30:3**,17-32, 2013.

[6] G. Mosqueda, A.S. Whittaker, G.L. Fenves, Characterization and modeling of friction pendulum bearings subjected to multiple components of excitation. *Journal of Structural Engineering*, **130**, 433-442, 2004.

[7] CEN, Comité Européen de Normalisation TC 340, *European Code UNI EN 15129:2009 Anti-seismic devices*. Brussels, 2009.

[8] F. Khoshnoudian, V.R. Hagdoust, Response of pure-friction sliding structures to three components of earthquake excitation considering variations in the coefficient of friction. *Scientia Iranica*, **16**, 429-442, 2009.

[9] M. Dolce, D. Cardone, F. C. Ponzo, A. Di Cesare, *Progetto di edifici con isolamento sismico, Seconda Edizione*. IUSS Press, 2010.

[10] D. Fenz, M. C. Constantinou, Behaviour of the double concave friction pendulum bearing. *Earthquake Engineering And Structural Dynamics*, **35**,1403–1424, 2006.

[11] A. K. Chopra, *Dynamics of Structures Theory and Applications to Earthquake Engineering*. Prentice Hall, Upper Saddle River, NJ, 1995.